

## Surface photoeffect for metals\*

K. L. Kliewer

*Ames Laboratory-ERDA and Department of Physics, Iowa State University, Ames, Iowa 50010*

(Received 15 October 1975)

A nonlocal theory for the surface photoeffect produced in metals by vacuum ultraviolet radiation is presented. Using a simple electron-gas model, it is shown that  $p$ -polarized incident light generates, in the surface region, a strongly spatially dependent vector potential having longitudinal character; it is argued that the photoemission associated with this longitudinal contribution constitutes the surface photoeffect. Various physical features, including the role of the optical constants and the nondirect nature of the electronic transitions involved, are discussed. It is shown that the nonlocal effects are significant over a wide range of frequencies and for systems other than the electron gas.

### I. INTRODUCTION

Among the more enduring problems in the world of photoemission is the surface photoeffect for metals.<sup>1-10</sup> In view of the many "surface effects" now being investigated with photoemission, I emphasize that the problem of concern here is the traditional surface photoeffect problem which may be stated as follows: What unique physical effects accompany the production of photoelectrons by  $p$ -polarized light? The standard for comparison implicit in this statement is the "bulk photoeffect"<sup>11-18b</sup> from which the surface effect must be disentangled when exciting with  $p$ -polarized light and which results when normally incident or  $s$ -polarized light is used. That which sets  $p$ -polarized light apart is the presence of an electric field component normal to the surface; the problem arises in assessing the consequences of this electric field component.

In generating a photoemission theory for metals, an essential ingredient is the proper treatment of the electromagnetic fields within the metal. An important step in this connection came with the realization that a significant longitudinal electric field is excited in the metal as a consequence of the normal electric field component when  $p$ -polarized light is incident upon the surface of the metal.<sup>19-28</sup> Excitation of photoelectrons by this longitudinal field represents an excitation mechanism which is unique to  $p$  polarization and which requires the presence of a surface. In my opinion, it is the surface photoeffect. The purpose of this paper is to examine the consequences of including the longitudinal field within the simple three-step model of photoemission, and to compare the results with the analogous theory when the longitudinal effects are ignored. A brief report of this work has already appeared.<sup>29</sup>

It should be noted that the present characterization of the surface photoeffect differs signifi-

cantly from the traditional approach wherein the requisite momentum-nonconserving electronic transitions occur through the appearance of the derivative of the surface potential with respect to the coordinate normal to the surface within the matrix elements. That is, for a semi-infinite photoemitter, the relevant matrix elements are of the form<sup>9</sup>

$$(\hat{\epsilon} \cdot \hat{z}) \int_{-\infty}^{\infty} \phi^{>*(k_{fz}, z) \left( \frac{dV}{dz} \right) \phi_i(k_{iz}, z) dz, \quad (1.1)$$

where the surface of the photoemitter lies near the plane  $z=0$ ,  $\phi^{>}(k_{fz}, z)$  is the  $z$ -dependent part of a wave function describing the excited photoemitted electron,  $\phi_i(k_{iz}, z)$  is the  $z$ -dependent part of the wave function describing the initial state of the electron,  $V$  is the potential function for the electrons with no external electromagnetic field present,  $\hat{\epsilon}$  is the polarization vector of the radiation within the photoemitter, and  $\hat{z}$  is a unit vector normal to the surface. The wave function  $\phi_i$  is associated with the  $z$ -direction wave-vector component  $k_{iz}$  while the part of  $\phi^{>}$  within the photoemitter is associated with the  $z$ -direction wave-vector component  $k_{fz}$ . If  $V$  is taken to be a step function at the surface, or even if the potential is softened somewhat from a step,  $dV/dz$  will be nonzero only in a narrow range very near the surface and the matrix element will be nonzero even if  $k_{fz} \neq k_{iz}$ , that is, the nonexistence of a momentum-conservation requirement in the direction normal to the surface due to the lack of translational invariance in this direction manifests itself right at the surface. The resulting photoemission will then represent a genuine surface effect and will occur only for  $p$ -polarized light. In the present work, the momentum required to couple crystal states having different momentum components normal to the surface comes from the longitudinal field which certainly arises as a consequence of the surface being present (and includes the effects of the lack of trans-

lational invariance), but which extends some tens of angstroms or even further into the photoemitter. Furthermore, this field derives its character largely from the bulk electronic excitations of the system. Thus, the surface photoeffect which emerges from the present study, while involving nondirect transitions and requiring  $p$ -polarized light as in the traditional picture, is more properly described as a hybrid excitation process having both surface and bulk character; no matrix elements of the form (1.1) are present. This dual character, appearing also in the work of Feibelman<sup>30</sup> and, to some extent, in the theory of En-driz,<sup>31</sup> will be more carefully discussed below.

In Sec. II, I describe the electron gas model which will be used for the calculation and generate a rather different photoemission theory. An extension of the theory to incorporate, in a simple way, non-electron-gas effects is also included. The results for the electron gas are presented in Sec. III. Section IV includes the results of some calculations based upon rather high-energy ( $\approx 50$  eV) photoemission data taken by Arakawa. The point of these calculations is to show that the inclusion of the effects associated with the longitudinal field modifies significantly the conclusions obtained from a simple scheme for the determination of electron escape lengths. A discussion of the reasons the present approach was employed and a comparison with alternative approaches is given in Sec. V.

## II. NONLOCAL THEORY AND THE LOCAL LIMIT

### A. Local limit

I consider  $p$ -polarized light of frequency  $\omega$  incident through a nonabsorbing medium of dielectric constant  $\epsilon_0$  upon a half-space photoemitter. Let us initially examine the local limit within the isotropic-volume-excitation model of photoemission<sup>32</sup> and thus characterize the photoemitter by the dielectric function  $\epsilon(\omega) = \epsilon_1(\omega) + i\epsilon_2(\omega)$ . This local limit has already been examined in detail<sup>33-35</sup>; however, an understanding of the photoemission ideas appearing therein is important for our subsequent development so we sketch the theory here. The reflectance  $R_{p,L}$  and absorptance  $A_{p,L}$  for the system are given by

$$\begin{aligned} R_{p,L} &= |(\cos\theta/\epsilon_0^{1/2} - Z_{p,L})/(\cos\theta/\epsilon_0^{1/2} + Z_{p,L})|^2 \\ &= 1 - A_{p,L}, \end{aligned} \quad (2.1)$$

where  $\theta$  is the incident angle, measured from the normal, in the medium of dielectric constant  $\epsilon_0$ , and the local surface impedance  $Z_{p,L}$  is  $Z_{p,L} = (\epsilon - \epsilon_0 \sin^2\theta)^{1/2}/\epsilon$ . We choose the surface of the photoemitter to be the plane  $z=0$ , with  $z$  increasing

into the photoemitter. The absorbed energy can then be described by

$$A_{p,L} = \int_0^\infty \frac{dA}{dz} dz,$$

with the distribution of this energy given by  $dA/dz = \alpha A_{p,L} e^{-\alpha z}$ . The absorption coefficient  $\alpha$  is  $\alpha = (2\omega/c) \text{Im}(\epsilon - \epsilon_0 \sin^2\theta)^{1/2}$ , with  $\text{Im}$  denoting the imaginary part.

We now assume that all the energy absorbed goes into single-electron excitations. The number of excited electrons produced within  $dz$  at  $z$  per incident photon is then  $(dA/dz)dz$ . If the probability that an excited electron produced at  $z$  will reach the surface is  $P(z) = \frac{1}{2}e^{-z/\xi}$ , the number of electrons reaching the surface per incident photon will be  $n_s$ ,

$$n_s = \int_0^\infty \frac{dA}{dz} \frac{e^{-z/\xi}}{2} dz. \quad (2.2)$$

The quantity  $\xi$ , the electron escape length, will in fact be a function of the final-state energy  $E_e$  of the excited electron. For simplicity, we consider here  $\xi$  to be an average escape length for excitation at frequency  $\omega$ . Then,

$$n_s = \frac{1}{2} A_{p,L} [\alpha\xi/(1 + \alpha\xi)]. \quad (2.3)$$

The local photoyield  $Y_{T,L}(\theta, \omega)$  can be written as the product of  $n_s$  and the transmission function describing the probability of escape of excited electrons at the surface. We will focus our attention here on the quantity  $2n_s$  which will call the local surface yield  $Y_L$ ,

$$Y_L(\theta, \omega) = A_{p,L} [\alpha\xi/(1 + \alpha\xi)]. \quad (2.4)$$

Caution must be exercised in using  $Y_L$  to describe the actual photoyield. In addition to the nonlocal effects, of which much will be said below, the surface escape function has been omitted; this function will be of prime importance in determining the yield, particularly for low and moderate energies. Now, the surface escape function depends upon the work function, the energy of the excited electron, and, equally importantly, upon the velocity of the excited electron in the direction normal to the surface. Thus, the details of the electron excitation spectrum, implicit in  $A_{p,L}$  and  $\alpha$ , are needed, together with the orientation of the crystal with respect to the incident light, before the escape function can be specified and the total photoyield given. For higher energies,  $\hbar\omega$  greater than several times the Fermi energy, say, these restrictions become less important and the spatially isotropic excitation character tacit in the above development is more nearly realized. In this case, characterizing the yield via  $Y_L$  (or its nonlocal generalization) becomes

more reasonable. Finally, we would like to point out that Eq. (2.4) includes the features of the more elaborate Berglund-Spicer development<sup>13</sup> in the limit that  $\alpha\xi \ll 1$ , the normal situation in a metal.

With an eye on the nonlocal model to be presented below, we note that (2.4) can be rewritten. If the photoemitter contains an electric field  $\vec{E}$  giving rise to a current density  $\vec{J}$ , the time-averaged power absorbed by the photoemitter per unit volume is  $\frac{1}{2} \text{Re}(\vec{J} \cdot \vec{E}^*)$ , with Re denoting the real part and the asterisk indicating the complex conjugate. Dividing this by the time-averaged energy flux incident upon the photoemitter,  $(c \cos\theta)/8\pi\epsilon_0^{1/2}$ , where we have taken the incident electric field in the lossless dielectric to have magnitude  $\epsilon_0^{-1/2}$  [see Eqs. (2.7) below], we have

$$\frac{dA}{dz} = \frac{4\pi\sqrt{\epsilon_0}}{c \cos\theta} \text{Re}(\vec{J} \cdot \vec{E}^*). \quad (2.5)$$

Since the fields and currents will have the form  $\vec{F}(z) e^{iq_x x}$ , where  $q_x = \omega\epsilon_0^{1/2} \sin\theta/c$ , and we have taken the light to be incident in the  $x$ - $z$  plane, the surface yield  $Y$  becomes

$$Y = \frac{4\pi\epsilon_0^{1/2}}{c \cos\theta} \int_0^\infty e^{-z/\xi} \text{Re}[\vec{J}(z) \cdot \vec{E}^*(z)] dz, \quad (2.6)$$

where  $Y$  without a subscript can be either a local or a nonlocal quantity. In the local limit, (2.12) is just (2.10). However, (2.12) is not restricted to the local limit and shall be used in the nonlocal theory which we sketch now.

### B. Nonlocal theory

There have appeared several variations of a nonlocal optical theory for  $p$ -polarized light incident upon a half-space electron gas with a surface which scatters the internal electrons specularly.<sup>36</sup> We will base our treatment here on the theory of Fuchs and Kliewer<sup>24, 25</sup> as this version contains the nonlocal effects associated with the collective excitations (plasmons) as well as with the single-particle excitations, the latter, as we will see, of considerable importance in the present context. This form of the nonlocal theory for the electron gas involves the bulk, frequency and wave-vector dependent, transverse and longitudinal dielectric functions as a consequence of the symmetry associated with the specular scattering condition. In this model the ground-state charge density is uniform up to the surface and thus the effects of charge rearrangement in the vicinity of the surface such as those recently discussed by Feibelman<sup>30</sup>

are not included. In addition, for the light incident upon the electron gas from vacuum, the electric field component normal to the surface is continuous across the surface and the current density component normal to the surface is zero at the surface, both results in marked contrast to the local situation. The continuity of the normal electric field at the surface points up one of the principle physical features of the nonlocal theory. It is the presence of a surface charge (polarization charge) layer which leads to the discontinuity of the normal component of the electric field in the local case. This charge layer is spread into the metal in the nonlocal description, the charge density is everywhere finite, and thus the fields have no discontinuities.

We are here taking the light to be incident through a lossless dielectric of dielectric function  $\epsilon_0$ . To treat the photoemitter nonlocally while retaining the local description of the outside dielectric is clearly an approximation; all dielectric functions are in fact nonlocal. For a dielectric which is a good insulator, the approximation should be reasonable. As a consequence of the locally described dielectric outside the photoemitter, the electric field component normal to the surface will no longer be continuous at the surface, the discontinuity arising from the polarization charge on the dielectric. We will comment further upon this and related points following the presentation of the basic equations.

Our coordinate system and dielectric-photoemitter arrangement are sketched in Fig. 1. Taking  $|\vec{E}_{\text{in}}| = \epsilon_0^{-1/2}$  and defining the reflectance amplitude to be  $r$ , we can write the fields in the dielectric due to the incident and reflected light as

$$E_x(x, z, t) = (\cos\theta/\epsilon_0^{1/2})(e^{ik_z z} - r e^{-ik_z z}) e^{iq_x x} e^{-i\omega t}, \quad (2.7a)$$

$$E_z^0(x, z, t) = (\sin\theta/\epsilon_0^{1/2})(e^{ik_z z} + r e^{-ik_z z}) e^{iq_x x} e^{-i\omega t}, \quad (2.7b)$$

and

$$H_y^0(x, z, t) = (e^{ik_z z} + r e^{-ik_z z}) e^{iq_x x} e^{-i\omega t}, \quad (2.7c)$$

with  $r = r_L$  in the local case and  $r = r_{\text{NL}}$  for the nonlocal case. Also,

$$q_x = (\omega\epsilon_0^{1/2}/c) \sin\theta \quad (2.8a)$$

and

$$k_z = (\omega\epsilon_0^{1/2}/c) \cos\theta. \quad (2.8b)$$

From the development in Ref. 24, it follows directly that the field ratios within the photoemitter are

$$\frac{E_x(z)}{H_y(0)} = \frac{2i\omega}{\pi c} \int_0^\infty \frac{dq_z \cos(q_z z)}{q^2} \left( \frac{q_x^2}{(\omega^2/c^2)\epsilon_t(q, \omega)} + \frac{q_z^2}{(\omega^2/c^2)\epsilon_t(q, \omega) - q^2} \right) \quad (2.9a)$$

and

$$\frac{E_x(z)}{H_y(0)} = \frac{2\omega q_x}{\pi c} \int_0^\infty \frac{dq_z q_z \sin(q_z z)}{q^2} \left( \frac{1}{(\omega^2/c^2)\epsilon_t(q, \omega) - q^2} - \frac{1}{(\omega^2/c^2)\epsilon_l(q, \omega)} \right), \quad (2.9b)$$

where the field components given, depending only on  $z$ , are the actual field components with the factor  $\exp[i(q_x x - \omega t)]$  removed. In Eqs. (2.9),  $q_x$  is given by (2.8a),  $q^2 = q_x^2 + q_z^2$ ,  $q_z$  is the wave vector normal to the surface,  $\epsilon_l(q, \omega)$  is the longitudinal dielectric function,  $\epsilon_t(q, \omega)$  is the transverse dielectric function, and  $H_y(0)$  is the magnetic field at the surface. The surface impedance  $Z_{p, NL}$  is defined by

$$Z_{p, NL} = E_x(0)/H_y(0) \quad (2.10)$$

and  $r_{NL}$ , the nonlocal reflectance amplitude, is

$$r_{NL} = \frac{\cos\theta/\epsilon_0^{1/2} - Z_{p, NL}}{\cos\theta/\epsilon_0^{1/2} + Z_{p, NL}}. \quad (2.11)$$

Since

$$H_y(0) = 1 + r_{NL}, \quad (2.12)$$

the optical properties are now determined if  $\epsilon_i$  and  $\epsilon_t$  are known.

For the electron gas, an appropriate longitudinal dielectric function to use is the generalized self-consistent-field expression  $\epsilon_{i, M}$  given by Mermin.<sup>37</sup> We are interested here in rather high frequencies,  $\omega \geq 0.1\omega_p$ , where  $\omega_p$  is the plasma frequency,  $\omega_p = (4\pi ne^2/m)^{1/2}$ , with  $n$  the electron density,  $m$  the electron mass, and  $e$  the magnitude of the electronic charge. With negligible loss of accuracy,<sup>38</sup> one may then use instead of the generalized self-consistent-field transverse dielectric function,<sup>39</sup> the local limit thereof,  $\epsilon(\omega)$ , given by

$$\begin{aligned} \epsilon(\omega) &= \lim_{q \rightarrow 0} \epsilon_{i, M}(q, \omega) = \lim_{q \rightarrow 0} \epsilon_t(q, \omega) \\ &= 1 - \omega_p^2/\omega(\omega + i/\tau), \end{aligned} \quad (2.13)$$

with  $\tau$  the mean electron lifetime which also appears in  $\epsilon_{i, M}$ .

We wish now to extend the model to include in a rough way non-electron-gas effects. Suppose we consider a system containing  $s$  electrons, which we consider to be essentially free and  $d$  electrons in rather flat bands. A useful approximation might than be to treat the  $s$  electrons (better, the "free" electrons) nonlocally and the  $d$  electrons (better, the "nonfree" electrons) locally, the longitudinal dielectric function then being of the form

$$\epsilon_{i, T}(q, \omega) = \epsilon_{ex}(\omega) + [\epsilon_{i, M}(q, \omega) - 1]. \quad (2.14)$$

Here  $\epsilon_{i, M}$  represents the free electrons of density  $n_f$  and, perhaps, with an effective mass differing from the actual free-electron value, while  $\epsilon_{ex}(\omega)$  is the local contribution due to the nonfree electrons, in general, a complex quantity. To recover the electron-gas result, we must take  $\epsilon_{ex}(\omega) = 1$ . Describing all nonfree electrons as strictly local is clearly an oversimplification. However, such a description can simulate the principal features in some complicated systems for which proper dielectric functions are very difficult to obtain.<sup>40(a)</sup>

Writing  $\epsilon_{i, T}$  in this form has significant consequences for the fields, particularly near the surface, as we now demonstrate. If our system is homogeneous or has cubic symmetry, the local dielectric function, now denoted  $\epsilon_T(\omega)$ , is the  $q \rightarrow 0$  limit of  $\epsilon_{i, T}$  or

$$\epsilon_T(\omega) = \epsilon_{ex}(\omega) - \omega_{p, f}^2/\omega(\omega + i/\tau_f), \quad (2.15)$$

where  $\omega_{p, f}$  is the plasma frequency of the free electrons which have a mean lifetime  $\tau_f$ . In addition,

$$\epsilon_{i, T}(\infty, \omega) = \lim_{q \rightarrow \infty} \epsilon_{i, T}(q, \omega) = \epsilon_{ex}. \quad (2.16)$$

Note that  $\epsilon_{i, T}(\infty, \omega) \neq 1$ , as it is for the electron-gas expression  $\epsilon_{i, M}$ . Using  $\epsilon_T(\omega)$  for  $\epsilon_t(q, \omega)$  in Eqs. (2.9) means that the integrals involving  $\epsilon_t$  can be done analytically. The field ratios can then be written

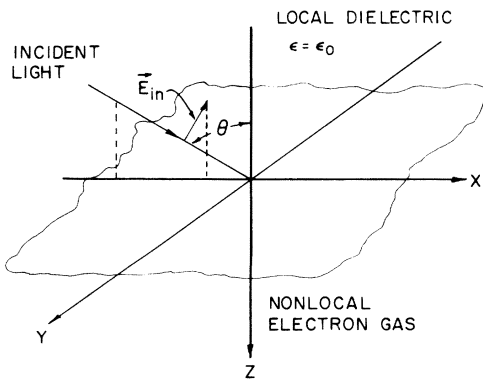


FIG. 1. Coordinate system and the dielectric-photoemitter arrangement. The light is incident in the local dielectric (of dielectric constant  $\epsilon_0$ ) at angle  $\theta$ . Within the local dielectric, the incident electric field for  $p$ -polarized light is indicated by  $\vec{E}_{in}$ .

$$\frac{E_x(z)}{H_y(0)} = \frac{(\epsilon_T - \epsilon_0 \sin^2 \theta)^{1/2}}{\epsilon_T} e^{i(\omega/c)(\epsilon_T - \epsilon_0 \sin^2 \theta)^{1/2} z} + i \left( \frac{1}{\epsilon_{ex}} - \frac{1}{\epsilon_T} \right) \sin \theta \epsilon_0^{1/2} e^{-q_x z} \\ + \frac{2i\omega}{\pi c} \epsilon_0 \sin^2 \theta \int_0^\infty dq_z \frac{\cos q_z z}{q^2} \left( \frac{1}{\epsilon_{i,T}(q, \omega)} - \frac{1}{\epsilon_{ex}(\omega)} \right) \quad (2.17a)$$

and

$$\frac{E_x(z)}{H_y(0)} = -\frac{\sin \theta \sqrt{\epsilon_0}}{\epsilon_T} e^{i(\omega/c)(\epsilon_T - \epsilon_0 \sin^2 \theta)^{1/2} z} - \epsilon_0^{1/2} \sin \theta \left( \frac{1}{\epsilon_{ex}} - \frac{1}{\epsilon_T} \right) e^{-q_x z} \\ - \frac{2 \sin \theta \epsilon_0^{1/2}}{\pi} \int_0^\infty dq_z \frac{q_z \sin(q_z z)}{q^2} \left( \frac{1}{\epsilon_{i,T}(q, \omega)} - \frac{1}{\epsilon_{ex}} \right). \quad (2.17b)$$

In the local limit  $\epsilon_{i,T} \rightarrow \epsilon_T$  and thus we obtain only the first terms of Eqs. (2.17) as we must.

Consider now the nonlocal situation, and in particular  $E_x(z)/H_y(0)$ , as  $z \rightarrow 0$ . The term containing the integral is then zero and we have

$$E_x(0)/H_y(0) = -\sin \theta \epsilon_0^{1/2} / \epsilon_{ex} \quad (2.18)$$

or<sup>40b</sup>

$$E_x(0) = -(\sin \theta \epsilon_0^{1/2} / \epsilon_{ex})(1 + \gamma_{NL}). \quad (2.19)$$

Comparing with Eq. (2.7b), we see that the continuity equation across the surface for the  $z$  component of the field is

$$\epsilon_0 E_{z,NL}^0(0) = \epsilon_{ex} E_{z,NL}(0), \quad (2.20)$$

where  $E_{z,NL}(0)$  is the nonlocal field component just within the photoemitter and  $E_{z,NL}^0(0)$  the field component just outside the photoemitter. Equation (2.20) is the nonlocal replacement for the local requirement that the displacement  $D$  be continuous in the direction normal to the surface. If we for the moment take  $\epsilon_0 = 1$ , then  $E_x$  will be continuous across the surface only if  $\epsilon_{ex} = 1$ . So, there will be no surface-charge layer for a system in vacuum only if  $\epsilon_i(q, \omega) \rightarrow 1$  as  $q \rightarrow \infty$ .

The local  $D$ -continuous condition analogous to (2.20) is

$$\epsilon_0 E_{z,L}^0(0) = \epsilon_T E_{z,L}(0) = \left( \epsilon_{ex} - \frac{\omega_{p,t}^2}{\omega(\omega + i/\tau_f)} \right) E_{z,L}(0), \quad (2.21)$$

with  $E_{z,L}(0)$  the electric field component just within the photoemitter in the local description, and  $E_{z,L}^0(0)$  the field component just without. Since  $E_{z,L}^0(0)$  and  $E_{z,NL}(0)$  are in practice not very different, it is apparent from (2.20) and (2.21) that  $E_{z,L}(0)$  and  $E_{z,NL}(0)$  can be very different and this difference will be seen to have significant effects on the photoemission.

Since we wish to use (2.6) to investigate the surface yield, we need also expressions for the cur-

rent density components. These will be obtained by using the procedure of Ref. 24. The Fourier transforms  $\mathcal{J}_x(q, \omega)$  and  $\mathcal{J}_z(q, \omega)$  of the current density components  $J_x(z)$  and  $J_z(z)$  can be written in a form identical to that used for the Fourier-transformed displacement components. Thus,

$$\mathcal{J}_x = \sigma_{xx} \mathcal{E}_x + \sigma_{xz} \mathcal{E}_z \quad (2.22)$$

and

$$\mathcal{J}_z = \sigma_{zx} \mathcal{E}_x + \sigma_{zz} \mathcal{E}_z, \quad (2.23)$$

where the  $\mathcal{E}$ 's are the Fourier transforms of the electric field components and the conductivity tensor elements are

$$\sigma_{xx} = (1/q^2)(\sigma_t q_z^2 + \sigma_l q_x^2), \quad (2.24)$$

$$\sigma_{zz} = (1/q^2)(\sigma_t q_x^2 + \sigma_l q_z^2), \quad (2.25)$$

and

$$\sigma_{xz} = \sigma_{zx} = (q_x q_z / q^2)(\sigma_l - \sigma_t). \quad (2.26)$$

The transverse conductivity  $\sigma_t$  and the longitudinal conductivity  $\sigma_l$  are defined in terms of the associated dielectric functions by

$$\epsilon_{i,t} = 1 + 4\pi i \sigma_{i,t} / \omega, \quad (2.27)$$

and the various  $q$ 's are defined in Eq. (2.8a) and following Eq. (2.9b). It is then a matter of manipulation to put the Fourier-transformed current densities into the forms

$$\frac{\mathcal{J}_x}{H_y(0)} = \frac{\omega^2}{2\pi c q^2} \left( \frac{q_x^2 (\epsilon_t - 1)}{(\omega^2/c^2) \epsilon_t} + \frac{q_z^2 (\epsilon_t - 1)}{(\omega^2/c^2) \epsilon_t - q^2} \right) \quad (2.28)$$

and

$$\frac{\mathcal{J}_z}{H_y(0)} = \frac{\omega^2 q_x q_z}{2\pi c q^2} \left( \frac{\epsilon_t - 1}{(\omega^2/c^2) \epsilon_t} - \frac{\epsilon_t - 1}{(\omega^2/c^2) \epsilon_t - q^2} \right). \quad (2.29)$$

Taking the inverse Fourier transforms, we obtain for the  $z$ -dependent parts of the current density components

$$\frac{J_x(z)}{H_y(0)} = \frac{\omega^2}{2\pi^2 c} \int_0^\infty dq_z \frac{\cos(q_z z)}{q^2} \left( \frac{q_x^2(\epsilon_i - 1)}{(\omega^2/c^2)\epsilon_i} + \frac{q_z^2(\epsilon_i - 1)}{(\omega^2/c^2)\epsilon_i - q^2} \right) \quad (2.30)$$

and

$$\frac{J_z(z)}{H_y(0)} = \frac{i\omega^2 q_x}{2\pi^2 c} \int_0^\infty dq_z \frac{q_z \sin(q_z z)}{q^2} \left( \frac{\epsilon_i - 1}{(\omega^2/c^2)\epsilon_i} - \frac{\epsilon_i - 1}{(\omega^2/c^2)\epsilon_i - q^2} \right). \quad (2.31)$$

Let us now use the dielectric functions introduced above for the electric fields, that is, for  $\epsilon_i$  we use  $\epsilon_{i,T}$  of Eq. (2.14) and for  $\epsilon_t$ ,  $\epsilon_T(\omega)$  of Eq. (2.15). Then,

$$\begin{aligned} \frac{J_x(z)}{H_y(0)} = & \frac{i\omega(\epsilon_T - 1)(\epsilon_T - \epsilon_0 \sin^2 \theta)^{1/2}}{4\pi\epsilon_T} e^{i(\omega/c)(\epsilon_T - \epsilon_0 \sin^2 \theta)^{1/2} z} + \frac{\omega\epsilon_0^{1/2} \sin \theta}{4\pi} e^{-q_x z} \left( \frac{1}{\epsilon_T} - \frac{1}{\epsilon_{ex}} \right) \\ & - \frac{q_x^2 c}{2\pi^2} \int_0^\infty dq_z \frac{\cos(q_z z)}{q^2} \left( \frac{1}{\epsilon_{i,T}(q, \omega)} - \frac{1}{\epsilon_{ex}} \right) \end{aligned} \quad (2.32a)$$

and

$$\begin{aligned} \frac{J_z(z)}{H_y(0)} = & \frac{i\omega(\epsilon_T - 1)\epsilon_0^{1/2} \sin \theta}{4\pi\epsilon_T} e^{i(\omega/c)(\epsilon_T - \epsilon_0 \sin^2 \theta)^{1/2} z} + \frac{i\omega\epsilon_0^{1/2} \sin \theta}{4\pi} e^{-q_x z} \left( \frac{1}{\epsilon_T} - \frac{1}{\epsilon_{ex}} \right) \\ & - \frac{i q_x c}{2\pi^2} \int_0^\infty dq_z \frac{q_z \sin(q_z z)}{q^2} \left( \frac{1}{\epsilon_{i,T}(q, \omega)} - \frac{1}{\epsilon_{ex}} \right). \end{aligned} \quad (2.32b)$$

As  $z \rightarrow 0$ , we have

$$\lim_{z \rightarrow 0} \frac{J_z(z)}{H_y(0)} = - \frac{i\omega\epsilon_0^{1/2} \sin \theta}{4\pi} \left( \frac{1}{\epsilon_{ex}} - 1 \right), \quad (2.33)$$

a result which does not depend upon the replacement of the transverse dielectric function by its local value. Note that  $J_z(0)$  is not zero at the surface unless  $\epsilon_{ex} = 1$ , that is, unless the longitudinal dielectric function  $\epsilon_{i,T}(q, \omega) \rightarrow 1$  as  $q \rightarrow \infty$ . So, even with a specular scattering model, the vanishing of the current density component normal to the surface at the surface is not assured. It is, of course, the local polarization effects which cause the right-hand side of (2.33) to be nonzero.

To calculate the nonlocal surface yield  $Y_{NL}$ , we must evaluate  $\vec{J}_{NL}$  and  $\vec{E}_{NL}$  from Eqs. (2.17) and (2.32) and then insert them into Eq. (2.6).

### III. SURFACE YIELDS FOR ELECTRON GAS IN VACUUM

To examine the surface yields for the electron gas in vacuum, we take  $\epsilon_0 = 1$  and  $\epsilon_{ex} = 1$ . The calculations have been made with the electron density of sodium so  $\hbar\omega_p = 6.07$  eV and the Fermi velocity  $v_F = 1.07 \times 10^8$  cm/sec. We have chosen the mean electron lifetime  $\tau = 10^9/\omega_p$  and defined  $\Omega = \omega/\omega_p$  and  $\gamma = (\omega_p \tau)^{-1}$ .

Before presenting the results, let us digress briefly and discuss the energy-loss function  $\text{Im}[-1/\epsilon_{i,M}(q, \omega)]$ , with  $\text{Im}$  denoting the imaginary part, a function which plays an important role in what is to follow. The energy-loss function characterizes the longitudinal excitations of the system, that is, it is nonzero for the values of  $\omega$  and  $q$  for which, in the present electron-gas case, elemen-

tary excitations of the electronic system can occur. In addition, its magnitude is a measure of the strength of the excitations.

Suppose that the frequency is less than the plasma frequency. The energy-loss function then contains only contributions from the region of single-particle excitations, which lies between the pair of parabolas<sup>41</sup>

$$\hbar\omega|_{10-q} = \hbar^2 k_F q/m + \hbar^2 q^2/2m \quad (3.1)$$

and

$$\hbar\omega|_{hi-q} = -\hbar^2 k_F q/m + \hbar^2 q^2/2m, \quad q \geq 2k_F. \quad (3.2)$$

Equation (3.1) yields the smallest allowable  $q$  for a given  $\omega$  (the "lo- $q$ " edge of the single-particle excitation region) while (3.2) yields the largest.

When  $\omega \geq \omega_p$  the plasmon enters the picture. Let us consider first  $1 < \Omega < \Omega_{LD}$ , where  $\Omega_{LD}$  is the frequency for which Landau damping sets in, or the frequency at which the plasmon dispersion curve enters the single-particle-excitation region. For the sodium parameters,  $\Omega_{LD} \approx 1.48$ . For  $\Omega$  fixed,  $\text{Im}(-1/\epsilon_{i,M})$  then has a large peak centered at the  $q$  of the plasmon dispersion curve and, for larger values of  $q$ , the broad single-particle region occurs. Finally, as  $\Omega$  increases beyond  $\Omega_{LD}$ , the plasmon occurs within the single-particle-excitation region and is strongly damped. Then  $\text{Im}(-1/\epsilon_{i,M})$  is nonzero only within the borders of the single-particle region but continues to show the remains of the plasmon out to frequencies well above  $\Omega_{LD}$ . An extensive discussion of  $\text{Im}(-1/\epsilon_{i,M})$  appears in Ref. 42.

Local and nonlocal surface yields are shown in Figs. 2 and 3 for two frequencies below the plasma frequency, namely,  $\Omega = 0.30$  and  $0.99$ , and a range

of electron escape lengths  $\xi$ . For  $\Omega = 0.30$  (Fig. 2), the nonlocal yields, which coincide with the local values for the same escape length at  $\theta = 0$ , rise significantly above their local counterparts as  $\theta$  increases. However, the shapes of the local and nonlocal curves are much the same. In particular, the maxima for the local and nonlocal cases lie at essentially the same angle for a given escape length.

It is the presence of the terms in  $\vec{E}$  and  $\vec{J}$  containing the longitudinal dielectric function  $\epsilon_{i, M}$  that leads to the enhancement of the nonlocal surface yields. To assess the effect of these terms, it is perhaps easiest to look at the absorptance for the system, which is roughly proportional to the real part of the surface impedance or  $\text{Re}[E_x(0)/H_y(0)]$ . From Eq. (2.17a) we then see that  $\epsilon_{i, M}$  contributes to the absorptance via the expression  $\text{Im}(-1/\epsilon_{i, M})/q^2$  in the integrand. Thus, the longitudinal effects occur through an integral over the energy-loss function multiplied by  $q^{-2}$ . Since we are now at a frequency  $\Omega < 1$ , the only contributions to the energy-loss function come from the single-particle excitations, and these excitations exist only for  $q$  values much larger than the wave vectors associated with photons. In Eq. (2.17a), this means that the  $q$  values which contribute to the integral are all such that  $q \approx q_x$ . Thus, the longitudinal contribution to the absorptance involves nondirect electronic transitions with the momentum transfer

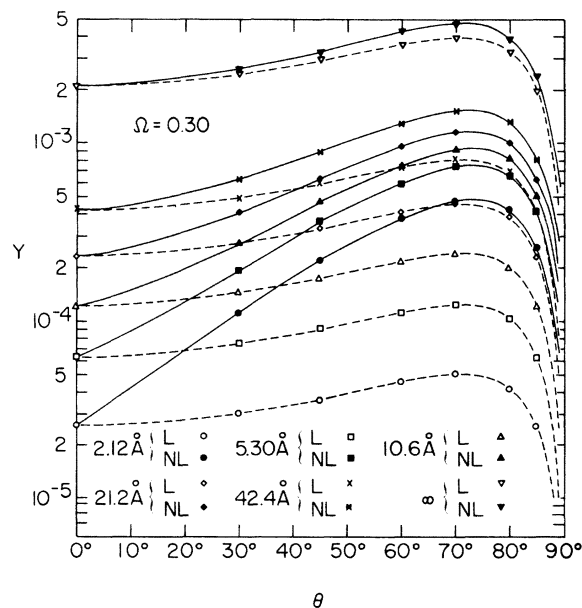


FIG. 2. Local and nonlocal surface yields for several electron escape lengths  $\xi$  as a function of the angle of incidence of the  $p$ -polarized light for  $\Omega = 0.30$ ,  $\gamma = 10^{-3}$ , and the sodium electron density.

essentially in the  $z$  direction, that is, normal to the surface. It is the longitudinal electric field, arising from the lack of translational invariance normal to the surface, which supplies the momentum necessary for the nondirect transitions to occur.

These same effects manifest themselves, of course, in  $dA/dz$  [Eq. (2.5)] and the integral giving the nonlocal yield [Eq. (2.6)]. However, some interesting new aspects emerge. The term in  $dA/dz$  coming from  $J_x E_x^*$  is very close to its local counterpart. This is not the case for the  $J_z E_z^*$  term which shows a strong damped-sinusoidal variation as a function of  $z$ ,<sup>29</sup> the origin of which can be understood as follows. All of the integrals above containing the longitudinal effects were written as integrals from  $q_x = 0 \rightarrow \infty$  with the integrands containing sinusoidal functions with argument  $q_x z$ . Since the dielectric functions are even functions of  $q$ , these integrals can also be written as integrals from  $q_x = -\infty \rightarrow \infty$  with the sinusoidal term then replaced by  $e^{iq_x z}$ . Since the integrands contain the energy-loss function divided by  $q^2$ , there will be a range of  $q$  values extending only a relatively short distance up from the low- $q$  edge

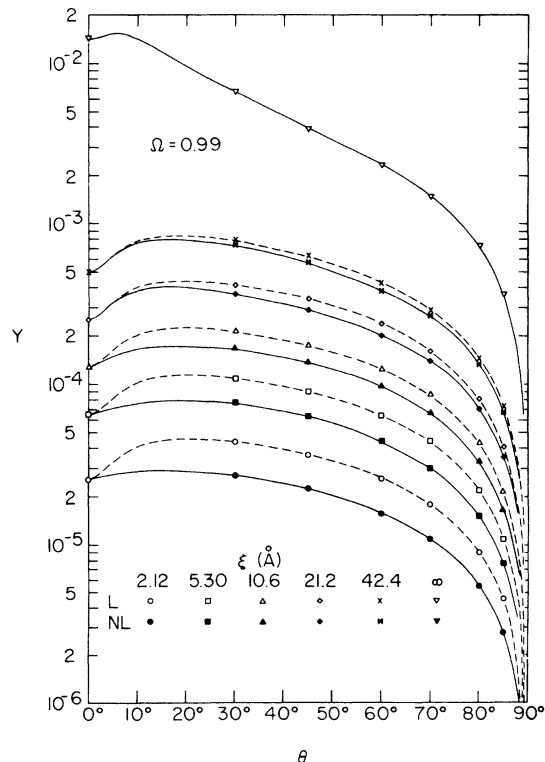


FIG. 3. Local and nonlocal surface yields for several electron escape lengths  $\xi$  as a function of the angle of incidence of the  $p$ -polarized light for  $\Omega = 0.99$ ,  $\gamma = 10^{-3}$ , and the sodium electron density.

of the single-particle-excitation region which will contribute effectively to the excitation spectrum, the higher- $q$  excitations essentially eliminated by the  $q^{-2}$  factor. Now, as is clear from the fact that the  $q_x$  integrals extend from  $-\infty$  to  $\infty$ , the incoming light, through the medium of the longitudinal field, produces, at a given value of  $z$ , excitations with both  $\pm q_x$ , that is, moving both toward and away from the surface. These excitation waves then interfere with each other and the result is the damped sinusoidal oscillations in  $dA/dz$ .<sup>43</sup> That the sinusoid is damped is a result of the spread of wave vectors excited, and, to a lesser extent, the finite lifetime  $\tau$ . Indeed, the distance into the system that the sinusoidal variation extends is roughly  $1/\Delta q$ , where  $\Delta q$  is the spread of wave vectors effective in producing the excitation spectrum. For  $\Omega = 0.3$ , the oscillation extends  $\sim 20 \text{ \AA}$  into the photoemitter with a wave length  $\sim 2\pi/q_{10-q}$ , where  $q_{10-q}$  is the  $q$  corresponding to the low- $q$  edge of the single-particle region. For larger  $z$ ,  $dA/dz$  in the nonlocal case is essentially that of the local result. Since the longitudinal effects are concentrated in the region  $\sim 20 \text{ \AA}$  from the surface, they will be most important for small escape lengths, and this is clearly indicated in Fig. 2.

Two points we would like to emphasize here. Although the longitudinal fields are restricted to the region near the surface, the electronic excitations from which these fields are comprised are the bulk electronic excitations, i.e., those which appear in  $\text{Im}(-1/\epsilon_{l, M})$ . This is the reason that we referred in the introduction to the hybrid character of the surface effect as here described. The second point is that, although the excitations produced at a given value of  $z$  move both toward and away from the surface, the net electric field at large  $z$  moves away from the surface as it must.

As the frequency increases to  $\Omega \sim 0.8$ , the basic character of the curves of Fig. 2 is preserved; the angle at which the maximum yield occurs decreases slowly with increasing frequency. A further increase to  $\Omega = 0.99$ , however, brings a striking change. The nonlocal yields shown in Fig. 3 are now below their local counterparts. This happens because we are now very near the plasma frequency, and hence, the local dielectric function  $\epsilon(\omega) \sim 0$ . The consequences of the small  $\epsilon$  can be assessed from several points of view. In the local theory, the displacement  $D$  normal to the surface must be continuous. Since we now have vacuum outside, this means that  $E_{\text{out}}(z=0) = \epsilon E_{L, \text{in}}(z=0)$ . (In this argument all fields are taken to be  $z$  components. The field components parallel to the surface are, of course, continuous across the surface.) In the nonlocal theory, on the other hand, the normal component of the field is continuous so

$E_{\text{out}}(z=0) = E_{NL, \text{in}}(z=0)$ . If we take  $E_{\text{out}}(z=0)$  as the same locally or nonlocally (not a bad approximation) this means that  $E_{L, \text{in}}(z=0) = E_{NL, \text{in}}(z=0)/\epsilon$  so  $|E_{L, \text{in}}(z=0)| \gg |E_{NL, \text{in}}(z=0)|$ . Now this is the situation right at the surface. To understand more completely what is happening, we must know over what range of  $z$  the nonlocal field is much smaller than the local. For large  $z$ , of course, the two must coincide.

Above, we discussed the fact that the resistive or absorptive aspect of the longitudinal effects was associated with the  $\text{Im}(-1/\epsilon_{l, M})$ . There will be for  $\Omega < 1$  also an essentially reactive part to the longitudinal field associated with  $\text{Re}(1/\epsilon_{l, M})$ . This reactive part contributes to the field  $E_x$  a longitudinal term which is approximately proportional to  $e^{iq_R z}$ , where

$$q_R^2 = \frac{\omega(\omega + i/\tau) - \omega_p^2}{\frac{3}{5} v_F^2 \omega_p^2 / \omega^2} \quad (3.3)$$

(The appropriate square root is the one with  $\text{Re } q_R > 0$  and  $\text{Im } q_R > 0$ .) This result follows directly from Eq. (2.17b). Let us write the low- $q$  expansion of  $\epsilon_{l, T}$  and then assert that the contri-

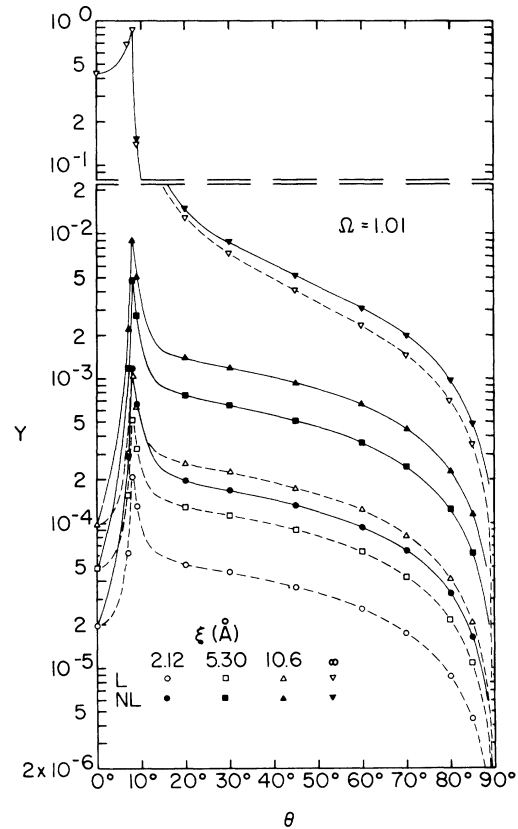


FIG. 4. Local and nonlocal surface yields for several electron escape lengths  $\xi$  as a function of the angle of incidence of the  $p$ -polarized light for  $\Omega = 1.01$ ,  $\gamma = 10^{-3}$ , and the sodium electron density.

bution to the integral from  $\epsilon_{i, T}$  occurs at that value of  $q_x$  associated with the pole  $\epsilon_{i, T} = 0$ . Making the argument for the electron gas ( $\epsilon_{i, T} = \epsilon_{i, M}$ ), we have, for  $qv_F \ll \omega$ ,

$$\epsilon_{i, M} |_{\text{small } q} \approx 1 - \frac{\omega_p^2}{\omega(\omega + i/\tau)} \left( 1 + \frac{3}{5} \frac{q^2 v_F^2}{\omega^2} \right). \quad (3.4)$$

For  $\epsilon_{i, M} |_{\text{small } q} = 0$ ,  $q = \pm q_R$ , with  $q_R$  given by Eq. (3.3). With  $\epsilon_{\text{ex}} = 1$ , the field ratio  $[E_x(z)/H_y(0)]$  then is

$$\frac{E_x(z)}{H_y(0)} = - \frac{\sin \theta \epsilon_0^{1/2}}{\epsilon(\omega)} e^{i(\omega/c)(\epsilon - \epsilon_0 \sin^2 \theta)^{1/2} z} + \frac{\epsilon_0^{1/2} \sin \theta}{\epsilon(\omega)} e^{iq_s z}, \quad (3.5)$$

where  $\epsilon$  is the local dielectric constant of Eq. (2.13) and

$$q_s = (q_R^2 - q_x^2)^{1/2}. \quad (3.6)$$

In the present case,  $q_x$  can in general be ignored in (3.6) so  $q_s \approx q_R$ .

The first term in (3.5) is the local transverse contribution to the field and the second term is the longitudinal part. Note that these fields are oppositely directed. From Eq. (3.5), the effect of the longitudinal contribution is clear. At  $z = 0$  it is large, so large in fact that within the present approximation the total field ratio is zero at the surface.<sup>44</sup> Because the imaginary part of  $q_s$  is so much larger than the absorption coefficient which characterizes the decay of the transverse field, the longitudinal term dies away much more rapidly than the transverse term leaving, for large  $z$ , only the transverse term. The region where the longitudinal term occurs is, of course, the region of nonzero charge density.

Clearly,  $q_R$  has both real and imaginary parts and thus is not associated with a purely reactive effect. However, it is the presence of  $\tau$  which introduces the resistive character; the large- $q$  resistive effects of the single-particle excitations are essentially  $\tau$  independent. For the sodium parameters and  $\gamma = (\omega_p \tau)^{-1} = 10^{-3}$ , the real and imaginary parts of  $q_R$  are given in Table I along with the inverse of the imaginary part of  $q_R$ . The real part of  $q_R$  is very small and not of significant interest. However, the inverse of the imaginary part of  $q_R$  is a measure of the distance over which the total field builds up as a consequence of the decay of the longitudinal field. This distance is very small until we get near the plasma frequency. For  $\Omega = 0.99$ , it is about 6 Å and this is indeed consistent with the results in Fig. 3.

An apparent dichotomy now arises. For lower frequencies we talked only of the resistive part of the longitudinal effects, and for  $\Omega = 0.99$  we

have referred only to the essentially reactive parts. The longitudinal field associated with  $e^{iq_R z}$  represents the essentially reactive, small- $q$  part of the total longitudinal field. It does not include the high- $q$  resistive parts of the longitudinal field which figure so prominently at lower frequencies and extend in general much further into the system. Indeed, approximating the longitudinal effects as we did in deriving Eq. (3.5) is totally inadequate if the absorptive effects associated with the longitudinal field are of interest as they are in photoemission.<sup>45</sup> It is only when the distance associated with the reactive field becomes reasonably big that its effects are important since a large distance portends a small total field in the surface region and thus a strong reduction in the photoyield for small to moderate escape lengths. This is an important effect which will manifest itself whenever the local limit of the longitudinal dielectric function is near zero but negative.<sup>46</sup>

Before leaving the region  $\Omega < 1$ , we would like to make two points. The first is that the theory as presented here contains no surface plasmon effects which can be of considerable importance if the surface is even slightly rough.<sup>34</sup> The second is to emphasize that we are dealing with a specular scattering model which perhaps is the surface model providing the weakest nonlocal effects. For diffuse scattering, for example, the nonlocal effects are far more pronounced in the single-particle-excitation region.<sup>47</sup>

We turn now to the frequency region  $\Omega > 1$ . In Fig. 4 is shown the angular dependence of the surface yield for  $\Omega = 1.01$ . The nonlocal surface yields are again well above the local and all curves have much the same shape. The fact that the local and nonlocal curves for a given value of  $\xi$  have similar shapes, here and for  $\Omega < 1$ , occurs since both  $\vec{J}$  and  $\vec{E}$  include both longitudinal and transverse terms and thus in an expression like  $J_x E_z^*$  there will be a transverse term, two mixed terms, and a longitudinal term. The purely longitudinal term is then added to a group of terms all of

TABLE I. Frequency dependence of  $q_R = q_R' + iq_R''$  and  $(q_R'')^{-1}$ . From the derivation it is apparent that  $q_R$  is a meaningful quantity only when  $|q_R| v_F / \omega \ll 1$ . The last column shows that this occurs only for  $\Omega$  very near one.

$\Omega$	$q_R = q_R' + iq_R''$ (cm <sup>-1</sup> )	$1/q_R''$ (Å)	$ q_R  v_F / \omega$
0.8	$5.93 \times 10^4 + i 5.34 \times 10^7$	1.87	0.77
0.9	$1.03 \times 10^5 + i 4.36 \times 10^7$	2.29	0.56
0.95	$1.61 \times 10^5 + i 3.30 \times 10^7$	3.03	0.40
0.97	$2.15 \times 10^5 + i 2.62 \times 10^7$	3.81	0.31
0.99	$3.86 \times 10^5 + i 1.55 \times 10^7$	6.44	0.18
0.999	$1.20 \times 10^6 + i 5.11 \times 10^6$	19.6	0.06

which have, at least in part, transverse character. It is the transverse character, or, in other words, an optical effect, which is principally responsible for the shape. For  $\omega > \omega_p$ , this optical effect can be described as follows.<sup>48</sup> For  $\theta = 0^\circ$ , the absorptance is high but the absorption coefficient is low so the yields are low. As  $\theta$  increases from  $0^\circ$ , the system is still highly absorbing, but the fields are refracted away from the normal since the index of refraction is between 0 and 1. Thus, the energy is refracted in such a way that it remains closer to the surface and the yields correspondingly increase. This increase persists until the critical angle  $\theta_c$ ,  $\theta_c \approx 8.1^\circ$  for  $\Omega = 1.01$ , where the refracted wave is moving parallel to the surface and the yields reach their maximum. As  $\theta$  increases beyond  $\theta_c$ , the system becomes strongly reflecting, the absorption coefficient increases but slowly so the product of the total absorptance and the absorption coefficient decreases and the yield decreases. These arguments are applicable for all  $\Omega > 1$ , and the same effects appear clearly in Fig. 5 for  $\Omega = 1.10$ , where  $\theta_c \approx 24.6^\circ$ , and also for  $\Omega = 1.414$ ,<sup>29</sup> where  $\theta_c = 45^\circ$ .

The enormous enhancement of the nonlocal sur-

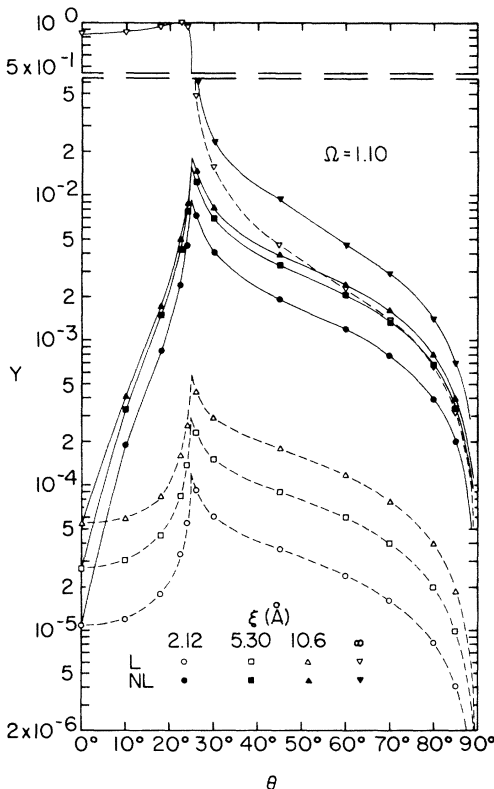


FIG. 5. Local and nonlocal surface yields for several electron escape lengths  $\xi$  as a function of the angle of incidence of the  $p$ -polarized light for  $\Omega = 1.10$ ,  $\gamma = 10^{-3}$ , and the sodium electron density.

face yields over the local values when  $\Omega > 1$  arises from plasmons excited by the longitudinal field. Since the plasmon is so sharply defined for the small damping used here, the energy-loss function is dominated by a sharp peak at  $q = q_p(\omega)$ , with  $q_p(\omega)$  the wave vector of the plasmon at frequency  $\omega$ . Since the peak is so sharp, the spread of wave vectors is small, and the interference effects which destroyed the longitudinal effects for  $\Omega < 1$  are essentially gone. Thus, the oscillation in  $dA/dz$  persists far into the system with a wavelength that of the plasmon.<sup>29</sup>

While the effects just discussed for  $\Omega > 1$  do indeed represent the optical situation, the same cannot be said for the photoemission. The plasmon is a collective excitation and can manifest itself in the photoemission only through decay into single-particle excitations. For the electron gas with  $\tau = \infty$  and  $\Omega < \Omega_{LD}$ , with  $\Omega_{LD}$  the frequency at which Landau damping sets in ( $\Omega_{LD} \approx 1.48$  for the present parameters), such decay cannot occur. For the large value of  $\tau$  in the present calculation, the plasmon damping, simulating weak interband effects, is very small. Thus, the nonlocal yields of Figs. 4 and 5 are in general too high. This, however, points up an interesting possibility. In real systems, plasmons can decay via interband transitions. So, for a given material, there may be crystallographic orientations where the plasmons decay easily giving rise to individual excited electrons. In such circumstances, the sharp increase in the yields as  $\Omega$  increases through 1.0 shown in Figs. 4 and 5 should indeed occur in the photoemission.

When  $\Omega > \Omega_{LD}$ , the above reservation concerning the role of the plasmons no longer exists. The plasmon is now heavily damped, what is left of it occurs in the single-particle-excitation region, and thus, it should contribute very effectively to the photoyield. Surface yields have been calculated for  $\Omega = 2.00$ ,<sup>49</sup> and 2.924; the latter are shown in Fig. 6. The interesting thing here is that these curves are so much like those for  $\Omega < \Omega_{LD}$ . While we expected the diffraction effects to persist essentially unchanged (the critical angle in Fig. 6 is  $70^\circ$ ) it is perhaps somewhat surprising that the enhancement of the nonlocal yield over the local, now due to single-particle excitations, is so large. The physical situation here is much like that described for  $\Omega = 0.3$  above. Because the longitudinal effects appear via  $\text{Im}(-1/\epsilon_{1,M})/q^2$ , the effective part of the single-particle-excitation region extends upward somewhat from the low- $q$  edge. As a result of this spread, there are interference effects and  $dA/dz$  is a damped sinusoid<sup>29</sup> extending about  $25 \text{ \AA}$  into the photoemitter with a wavelength roughly that corresponding to the low- $q$

edge of the single-particle region. Again, we emphasize that all these longitudinal effects are associated with nondirect electronic transitions.

To provide a somewhat different perspective on these results, we have shown in Figs. 7-9 the frequency dependence of the surface yield for a fixed angle. For  $\theta = 0^\circ$  (Fig. 7) the curves, purely local, reflect the product of the absorption coefficient and the total absorptance, reasonably large and constant for  $\Omega < 1$  and decreasing as  $\Omega$  increases from 1. When  $\theta = 45^\circ$ , Fig. 8 shows that for  $\Omega < 1$ , the nonlocal single-particle effects are strongest for  $\Omega \sim 0.6$ . Below this frequency they drop off because  $\text{Im}(-1/\epsilon_{l,M})$  is decreasing and above because of the  $q^{-2}$  multiplying the energy-loss function and also the effects of decreasing  $|\epsilon|$ , associated as it is with a reduced electric field near the surface. The sharp drop due to the small  $|\epsilon|$  as  $\Omega \rightarrow 1$  is very apparent as are the plasmon effects for  $\Omega > 1$ . As noted above, the region  $1.0 < \Omega < 1.48$  must be viewed with some care. Increasing  $\theta$  to  $70^\circ$  results in the yields shown in Fig. 9. Again, the frequency range of the essentially undamped plasmon,  $1.0 < \Omega < 1.48$ ,

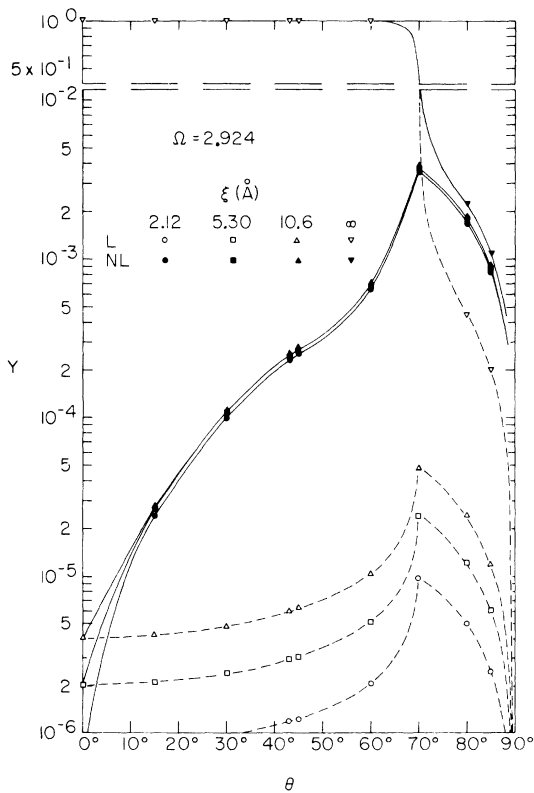


FIG. 6. Local and nonlocal surface yields for several electron escape lengths  $\xi$  as a function of the angle of incidence of the  $p$ -polarized light for  $\Omega = 2.924$ ,  $\gamma = 10^{-3}$ , and the sodium electron density.

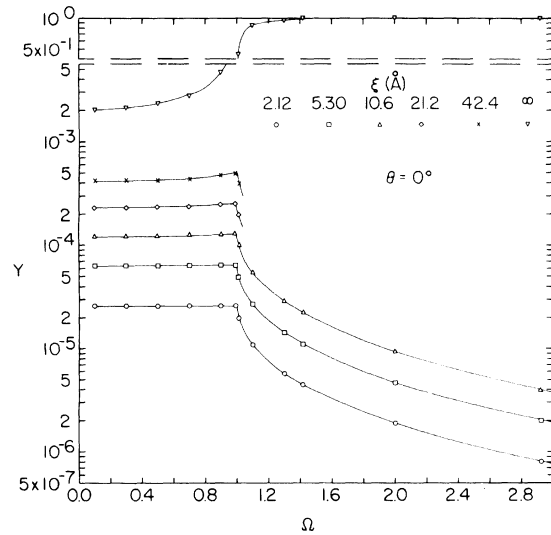


FIG. 7. Local surface yields for several electron escape lengths  $\xi$  as a function of the frequency for normally incident light and the electron density of sodium. Since  $\theta = 0$ , local and nonlocal surface yields for a given value of  $\xi$  are the same.

must be kept in mind.

One aspect of these results bears further comment. In situations where the plasmon is relatively weakly damped for  $1 < \Omega < \Omega_{LD}$  and contributing but little to the photoyield, there should occur a strong increase in the photoyield as  $\Omega$  passes through  $\Omega_{LD}$ . For situations where the plasmon is

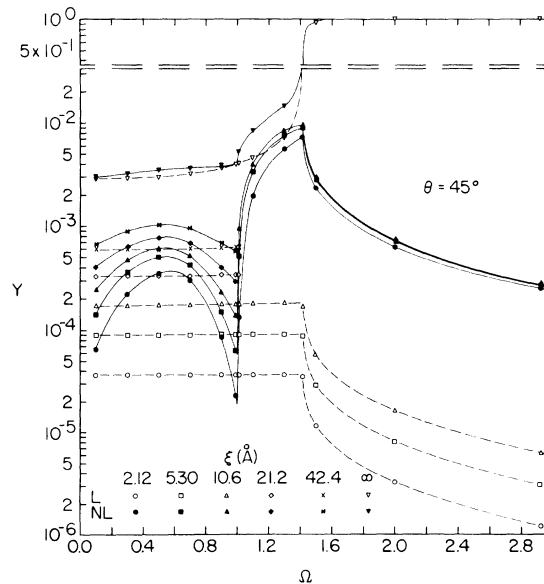


FIG. 8. Nonlocal and local surface yields for several electron escape lengths  $\xi$  as a function of the frequency of the incident  $p$ -polarized light for  $\theta = 45^\circ$ ,  $\gamma = 10^{-3}$ , and the electron density of sodium.

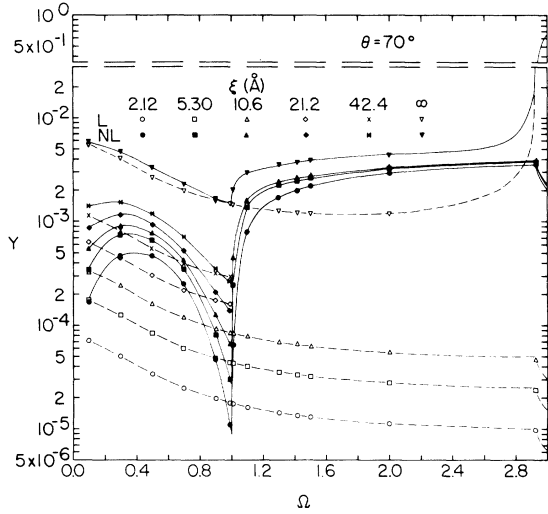


FIG. 9. Nonlocal and local surface yields for several electron escape lengths  $\xi$  as a function of the frequency of the incident  $p$ -polarized light for  $\theta = 70^\circ$ ,  $\gamma = 10^{-3}$ , and the electron density of sodium.

always rather strongly damped, it will contribute significantly to the photoyield as soon as  $\Omega > 1$ , and nothing dramatic should occur for  $\Omega \sim \Omega_{LD}$ .

We conclude this discussion of sodium with low damping by showing in Fig. 10 the integrated ab-

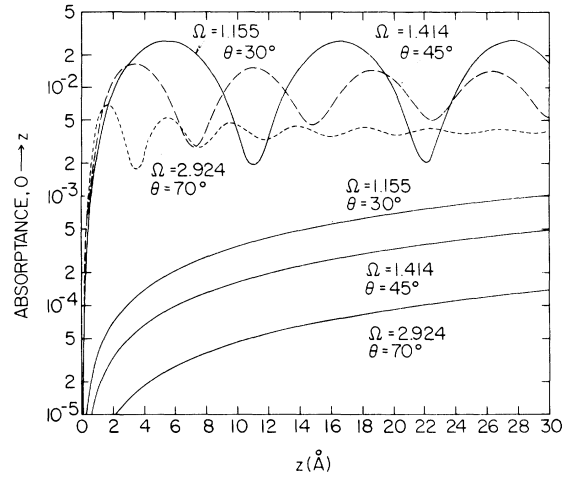


FIG. 10. The integrated absorbance  $A(z) = \int_0^z (dA/dz) dz$  as a function of  $z$ , for  $\gamma = 10^{-3}$ , the electron density of sodium, and several combinations of incident angle and frequency. The lower three curves are the local results and the upper three curves the nonlocal results.

sorbance for several frequencies and angles.<sup>50</sup> The total absorbance for the system is the value along the ordinate as  $z \rightarrow \infty$ . The effect of the oscillation in  $dA/dz$  is very clear, but perhaps as striking is the significant extent to which, for

TABLE II. Yield ratios for  $\Omega < 1$  and several values of  $\gamma$  and electron density. (Aluminum is here considered to be a free-electron gas with  $v_F = 2.03 \times 10^8$  cm/sec and  $\hbar\omega_p = 15.8$  eV.)  $Y_{p,L}(\theta)$  and  $Y_{p,NL}(\theta)$  are the local and nonlocal surface yields for  $p$ -polarized light incident at angle  $\theta$ .  $Y(0)$  is the surface yield for normally incident light for which the local and nonlocal yields are the same.  $Y_s(\theta)$  is the surface yield for  $s$ -polarized light incident at angle  $\theta$  and is given by Eq. (2.4) with  $A_{p,L}$  replaced by  $A_{s,L}$ , the total absorbance for  $s$  light, given by Eq. (4.4) below.

$\Omega$	$\theta = 60^\circ$	$\xi$ (Å)	Na ( $\gamma = 10^{-3}$ )				Na ( $\gamma = 10^{-2}$ )		Al ( $\gamma = 4 \times 10^{-2}$ )		
			$\frac{Y_{p,NL}(\theta)}{Y(0)}$	$\frac{Y_{p,NL}(\theta)}{Y_s(\theta)}$	$\frac{Y_{p,NL}(\theta)}{Y_{p,L}(\theta)}$	$\frac{Y_{p,NL}(\theta)}{Y(0)}$	$\frac{Y_{p,NL}(\theta)}{Y_s(\theta)}$	$\frac{Y_{p,NL}(\theta)}{Y_{p,L}(\theta)}$	$\frac{Y_{p,NL}(\theta)}{Y(0)}$	$\frac{Y_{p,NL}(\theta)}{Y_s(\theta)}$	$\frac{Y_{p,NL}(\theta)}{Y_{p,L}(\theta)}$
0.50	$60^\circ$	2.12	18.6	37.2	12.4	3.14	6.12	2.08	1.73	3.38	1.18
		5.30	10.8	21.6	7.21	2.39	4.68	1.59	1.60	3.14	1.09
		10.6	6.54	13.1	4.39	1.99	3.89	1.32			
		21.2	4.19	8.48	2.83	1.76	3.46	1.18			
		$\infty$	1.62	3.62	1.21	1.36	2.95	1.02	1.34	2.91	1.01
0.70	$60^\circ$	2.12	12.2	24.4	9.68	2.19	4.35	1.74	1.33	2.59	1.06
		5.30	6.85	13.8	5.48	1.73	3.45	1.38	1.28	2.51	1.03
		10.6	4.23	8.57	3.41	1.50	3.01	1.21			
		21.2	2.80	5.74	2.28	1.36	2.77	1.11			
		$\infty$	1.10	2.88	1.15	0.975	2.54	1.02	0.971	2.46	1.01
0.90	$60^\circ$	2.12	2.52	5.08	2.36	0.971	1.92	0.901	0.898	1.70	0.814
		5.30	1.75	3.56	1.66	0.988	1.97	0.925	0.967	1.87	0.893
		10.6	1.41	2.89	1.35	1.00	2.03	0.952			
		21.2	1.21	2.55	1.19	1.00	2.08	0.974			
		$\infty$	0.539	2.20	1.03	0.533	2.14	1.01	0.552	2.11	1.01
0.99	$60^\circ$	2.12	0.615	1.23	0.613	0.635	1.20	0.601	0.804	1.35	0.684
		5.30	0.684	1.39	0.691	0.721	1.39	0.692	0.916	1.58	0.804
		10.6	0.749	1.56	0.774	0.796	1.56	0.781			
		21.2	0.804	1.73	0.859	0.845	1.73	0.862			
		$\infty$	0.166	2.03	1.01	0.179	2.02	1.01	0.248	1.99	1.01

$\omega > \omega_p$ , the absorbed energy is concentrated near the surface nonlocally in contrast to the local results which are described by the ordinary absorption coefficient.

To illustrate the effect of increased damping we have given some surface yield ratios in Table II for  $\Omega < 1$  and in Table III for  $\Omega > 1$ . The Na ( $\gamma = 10^{-3}$ ) results are those shown in the figures. The  $Y_s$  are given by Eq. (2.10) with  $A_{p,L}$  replaced by the total absorptance for  $s$ -polarized incident light. While the relative importance of the nonlocal effects clearly diminishes as the damping increases, they can still be important for rather large damping, particularly for  $\Omega > 1$ . It should be kept in mind, however, that the single-particle effects will be considerably larger if the surface scattering of the internal electrons is other than specular.<sup>47</sup> It should also be noted that escape characteristics, not included here, can influence these conclusions. That is, if the nonlocally excited electrons are directed so as to be more likely to escape through the surface, their importance can exceed that indicated in the figures and tables.<sup>30,51</sup>

#### IV. NONLOCAL EFFECTS IN DETERMINATIONS OF ESCAPE LENGTHS

A scheme which has been proposed for the determination of electron escape lengths involves measurements of the total photoyield under two different illumination conditions,<sup>35,48,52,53</sup> e.g., measuring at a given frequency two among the

total yield for  $p$  light incident at angle  $\theta$ ,  $Y_{T,p}(\theta)$ , the total yield for  $s$  light incident at angle  $\theta$ ,  $Y_{T,s}(\theta)$ , and the total yield for normally incident light,  $Y_T(0)$ . By writing an expression for the ratio of two of these yields and assuming (i) the validity of the three-step model, (ii) the validity of the isotropic-volume-excitation model, and (iii) the nondependence of the escape characteristics on illumination conditions, it is possible to obtain an equation with the electron escape length  $\xi$  as the only unknown quantity and thus obtainable from the measured yield ratio. These schemes were generated from a strictly local point of view and a knowledge of the optical constants was presupposed.

Now, the assumptions upon which these schemes are based are certainly not valid for low or moderate energies, but appear more reasonable when  $\hbar\omega \gg E_F$ , the Fermi energy. It is our intention here to examine one such scheme, that of Arakawa *et al.*,<sup>48,53</sup> and show that the conclusions are significantly affected by the inclusion of nonlocal contributions to the yield when the incident light includes a  $p$ -polarized component.

Arakawa *et al.* use a thick photoemitter in vacuum and a partially plane-polarized incident beam with

$$P = I_p / I_s, \quad (4.1)$$

where  $I_p$  ( $I_s$ ) is the intensity of  $p$  ( $s$ ) light in the incident beam. They define the quantity  $Y(\theta)$  by

$$Y(\theta) = [Y_{T,s}(\theta) + PY_{T,p}(\theta)] / (1 + P). \quad (4.2)$$

TABLE III. Yield ratios for  $\Omega > 1$  and several values of  $\gamma$  and electron density. The various quantities are described in the caption of Table II. A digit in parenthesis is the power of 10 by which the preceding number should be multiplied.

$\Omega$	$\theta$	$\xi$ (Å)	Na ( $\gamma = 10^{-3}$ )				Na ( $\gamma = 10^{-2}$ )			Al ( $\gamma = 4 \times 10^{-2}$ )		
			$\frac{Y_{p,NL}(\theta)}{Y(0)}$	$\frac{Y_{p,NL}(\theta)}{Y_s(\theta)}$	$\frac{Y_{p,NL}(\theta)}{Y_{p,L}(\theta)}$	$\frac{Y_{p,NL}(\theta)}{Y(0)}$	$\frac{Y_{p,NL}(\theta)}{Y_s(\theta)}$	$\frac{Y_{p,NL}(\theta)}{Y_{p,L}(\theta)}$	$\frac{Y_{p,NL}(\theta)}{Y(0)}$	$\frac{Y_{p,NL}(\theta)}{Y_s(\theta)}$	$\frac{Y_{p,NL}(\theta)}{Y_{p,L}(\theta)}$	
1.155	2.12	2.12	989	402	118	74.8	32.9	11.9	12.9	6.48	3.11	
30°	5.30	5.30	592	241	70.5	47.9	21.1	7.66	8.93	4.50	2.16	
	10.6	10.6	335	132	38.7	28.7	12.7	4.66				
	∞	∞	0.415	3.52	1.03	0.745	2.79	1.01	0.972	2.09	1.01	
1.414	2.12	2.12	1590	398	205	138	37.7	21.0	26.2	8.08	4.98	
45°	5.30	5.30	785	196	101	71.2	19.5	10.8	14.8	4.59	2.83	
	10.6	10.6	420	105	54.1	39.7	10.9	6.07				
	∞	∞	1.27(-1)	2.08	1.07	0.389	1.82	1.02	0.640	1.64	1.01	
2.00	2.12	2.12	2580	382	290	241	38.3	29.6	44.8	7.90	6.30	
60°	5.30	5.30	1150	171	129	112	17.8	13.8	23.4	4.14	3.29	
	10.6	10.6	593	88.0	66.7	60.6	9.65	7.47				
	∞	∞	8.65(-2)	1.40	1.06	0.239	1.32	1.02	0.423	1.27	1.01	
2.924	2.12	2.12	4330	406	360	416	41.2	36.8	73.2	7.88	7.10	
70°	5.30	5.30	1860	174	154	185	18.3	16.3	36.5	3.95	3.55	
	10.6	10.6	942	88.4	78.4	98.1	9.73	8.69				
	∞	∞	7.29(-2)	1.19	1.05	0.177	1.14	1.02	0.319	1.13	1.02	

The purely local quantity  $Y_{T,s}(\theta)$  is given by

$$Y_{T,s}(\theta) = [A_{s,L} \alpha(\theta) \xi / (1 + \alpha \xi)] C, \quad (4.3)$$

where  $\alpha(\theta)$  is the absorption coefficient,

$$R_{s,L} = \left| \frac{1 - \cos \theta / (\epsilon - \sin^2 \theta)^{1/2}}{1 + \cos \theta / (\epsilon - \sin^2 \theta)^{1/2}} \right|^2 = 1 - A_{s,L}, \quad (4.4)$$

$\epsilon$  is the local dielectric constant of the photoemitter, and  $C$  is the escape probability for excited electrons which reach the surface, here taken to be a function only of  $\omega$ . Arakawa *et al.* take for  $Y_{T,p}(\theta)$  Eq. (2.4) multiplied by  $(2C)$ , but we will now allow  $Y_{T,p}(\theta)$  to be either the local expression used by Arakawa *et al.* or its nonlocal generalization, Eq. (2.6) (with  $\vec{J}$  and  $\vec{E}$  calculated nonlocally) multiplied by  $(2C)$ . Defining then

$$G(\theta) = Y(\theta)/Y(0), \quad (4.5)$$

$C$  cancels out. In the local picture we have left a function of the optical constants and  $\xi$ . Knowing the optical constants means that we can in principle obtain  $\xi$  from measurements of  $G(\theta)$ . In the nonlocal picture, the determination of  $\xi$  requires knowing the optical constants and having a model for the longitudinal dielectric function. In practice, Arakawa *et al.*, using only the local picture, employed a curve-fitting procedure to obtain  $\sqrt{\epsilon} = n + ik$  as well as  $\xi$  from a curve of  $G(\theta)$  as a function of  $\theta$ . We will use a simpler procedure to show the effects of nonlocality. This procedure is to use the  $n$  and  $k$  values determined by Arakawa *et al.* and then focus our attention upon the magnitude and angular position of the maximum in  $G(\theta)$ .

Let us consider first amorphous carbon. The values of  $n$ ,  $k$ , and  $P$  provided to me by Arakawa<sup>54</sup> for three energies are given in Table IV. All the information needed to make the local calculation is

TABLE IV. Optical constants,  $n$  and  $k$ , for amorphous carbon and the polarization factor  $P$  in the experiments of Arakawa *et al.* for three incident energies. The values of  $\omega_p$ ,  $\gamma$ ,  $v_F$ , and  $r_s$  given are the free-electron parameters resulting from the assumption that amorphous carbon can be considered a damped free-electron gas.

	64.30	$\hbar\omega$ (eV) 52.92	38.36
$n$	0.925	0.892	0.831
$k$	0.020	0.040	0.085
$P$	0.944	0.920	0.870
$\omega_p$ (eV)	25.3	25.4	23.7
$\gamma$	0.649	0.718	0.722
$v_F$ (cm/sec)	$2.77 \times 10^8$	$2.78 \times 10^8$	$2.65 \times 10^8$
$r_s$	1.51	1.51	1.58

now available. In order to generate a nonlocal longitudinal dielectric function  $\epsilon_l(q, \omega)$ , I assumed that  $\epsilon_l(0, \omega)$  was given by the damped free-electron form

$$\epsilon_l(0, \omega) = 1 - \omega_p^2 / \omega(\omega + i\omega_p \gamma),$$

with  $\gamma = (\omega_p \tau)^{-1}$ , took the electron mass to be the free-electron value, used the  $n$  and  $k$  values of Table IV, and obtained the results also shown in Table IV. The agreement in the free-electron parameters at the higher two energies is striking, suggesting that such a description in this energy range is indeed appropriate. However, the parameters change considerably in going to the lowest energy in Table IV, presumably the result of band-structure effects. Let us consider these energies in turn.

$\hbar\omega = 64.30$  eV. Arakawa<sup>54</sup> found the maximum in  $G(\theta)$  to be 7.02 at an angle of  $72^\circ$ . Doing the calculation locally using the parameters of Table IV,  $G(\theta)$  had a maximum value of 5.88 as  $\xi \rightarrow 0$  at an angle of  $71.3^\circ$ . It is thus impossible to find a  $G$  as large as the experimental value. Using the parameters of Table IV in the dielectric constant  $\epsilon_{l,M}$  and then doing the  $p$  part of the calculation nonlocally,  $G(\theta) = 7.02$  occurred for  $\xi = 0.9$  Å and  $\theta = 71.2^\circ$ . To put much faith in the actual result when  $\xi$  is so small is perhaps unwise. However, the fact that an experimental value which cannot be achieved in the local theory can with the nonlocal theory points to a significant improvement in the physical content of the nonlocal theory as compared with the local.

$\hbar\omega = 52.92$  eV. The experimental maximum in  $G(\theta)$  is 4.25 at an angle of  $69^\circ$ .<sup>54</sup> In the local calculation, this maximum value of  $G(\theta)$  occurred for  $\xi = 1.9$  Å at an angle of  $67.9^\circ$  while the nonlocal result was  $\xi = 4.9$  Å at an angle of  $67.6^\circ$ . This nonlocal result appears to us considerably more reasonable.<sup>55,56</sup>

$\hbar\omega = 38.36$  eV. The experimental maximum in  $G(\theta)$  is 2.63 at an angle of  $62^\circ$ . Proceeding as above we now find that, locally or nonlocally, the value of  $\xi$  has risen to about 15 Å at an angle of about  $61.5^\circ$ . Such a sharp rise in this energy range is, in my opinion, unreasonable and may portend the breakdown of the assumptions made in this simple model. (Another possibility will be discussed just below in connection with some comments about silicon.) Since we are now at an energy of about  $1.6 \hbar\omega_p$ , with  $\omega_p$  the plasma frequency, band-structure effects should be reflected in the electron excitation spectrum and the escape characteristics, as they apparently are in the parameters of Table IV.

These results suggest that the simple model is perhaps valid for  $\hbar\omega \gtrsim 2(\hbar\omega_p)$ . Let us, however,

TABLE V. Optical constants,  $n$  and  $k$ , for silicon and the polarization factor  $P$  in the experiments of Arakawa *et al.* for two incident energies. Also given are the calculated dielectric function parameters  $\epsilon_{\text{ex}}$  and  $\gamma$ .

	$\hbar\omega$ (eV)	
	59.32	46.60
$n$	0.974	0.959
$k$	0.003	0.005
$P$	0.99	0.94
$\epsilon_{\text{ex}} - 1$	0.0266	0.0459
$\gamma$	0.268	0.213

now look at some results for polycrystalline silicon where the simple model appears to have no validity.

In Table V are the values of  $n$ ,  $k$ , and  $P$  obtained by Arakawa<sup>54</sup> for two energies in the range where we might expect the simple model to be valid. In this case, writing the local dielectric constant in the free-electron form was not successful so we chose the form (2.15a) and took  $\hbar\omega_{p,f} = 16.6$  eV, the value resulting from the assumption that the plasma oscillation involves four free electrons per atom. The resulting parameters are also shown in Table V. In calculating  $G(\theta)$  nonlocally, the longitudinal dielectric function was then taken to be Eq. (2.14). The maximum values of  $G(\theta)$  and the associated angles for several escape lengths are given in Table VI. The experimental results of Arakawa<sup>54</sup> were

$$\hbar\omega_p = 59.32 \text{ eV}, \quad G_{\text{max}} = 8.1 \text{ at } \theta_{\text{max}} = 77^\circ,$$

$$\hbar\omega_p = 46.60 \text{ eV}, \quad G_{\text{max}} = 6.4 \text{ at } \theta_{\text{max}} = 73^\circ.$$

To obtain the experimental values of  $G_{\text{max}}$  from the theory requires what appear to be excessively large escape lengths,<sup>55</sup> a possible explanation being, of course, that the simple model is totally deficient. There is, however, another possibility. When the  $G$  values are as large as they are here, the values of  $Y(0)$  are small and thus small absolute errors in  $Y(0)$  would have significant effects in  $G(\theta)$ . It is now well established that at low en-

ergies, yields from  $s$  light or normally incident light are extremely sensitive to the quality of the surface,<sup>57,58</sup> and, in general, increase considerably more rapidly than the  $p$  yields as the quality of the surface deteriorates.<sup>58</sup> If such an effect occurs also at higher energies, it might account for the seemingly too low experimental values of  $G(\theta)$  obtained for silicon.

## V. DISCUSSION OF PRESENT THEORY AND ALTERNATIVES

In the Introduction I commented that it is the effects associated with the longitudinal field that comprise the surface photoeffect. It is, perhaps, worthwhile to examine this statement more closely and, in the process, relate the present theory to the more conventional theory of photoemission.

The primary physical feature characterizing the surface photoeffect is, in my opinion, the existence of a vector potential which is a strong function of the distance from the surface in the region of the surface. The longitudinal field constitutes just such a contribution to the vector potential. Indeed, since the scalar potential can be taken to be zero, the vector potential  $\vec{A}$  in the present nonlocal theory is given by

$$\vec{A} = c\vec{E}/i\omega, \quad (5.1)$$

with  $\vec{E}$  the nonlocal electric field, and, as is clear from the above,  $\vec{A}$  is a strong function of the distance from the surface when the incident light is  $p$  polarized. Using the interaction

$$H_{\text{int}} = \frac{1}{2}(\vec{A} \cdot \vec{p} + \vec{p} \cdot \vec{A}) \quad (5.2)$$

in the matrix elements of the standard photoemission theories then means that it is impossible, because of the  $z$  dependence of  $H_{\text{int}}$ , to generate an expression like (1.1); conclusions drawn from a theory which describes the surface effect via expressions like (1.1) must be suspect.

The theory presented here includes the effects of the spatial dependence of  $\vec{A}$ . Have we then provided a comprehensive theory of the surface photoeffect? The answer is no, and in seeking im-

TABLE VI. Calculated values of  $G_{\text{max}}$ , the maximum value of  $G(\theta)$ , and the angle  $\theta_{\text{max}}$  for which  $G_{\text{max}}$  occurs for silicon at two incident energies. The dielectric function parameters used in the calculations are given in Table V.

	$\hbar\omega = 59.32$ eV				$\hbar\omega = 46.60$ eV				
	Local		Nonlocal		Local		Nonlocal		
	$G_{\text{max}}$	$\theta_{\text{max}}$	$G_{\text{max}}$	$\theta_{\text{max}}$	$G_{\text{max}}$	$\theta_{\text{max}}$	$G_{\text{max}}$	$\theta_{\text{max}}$	
$\xi$ (Å)	1	12.5	78.2	24.0	78.2	9.85	75.3	17.5	75.1
	3	12.4	78.2	16.6	78.2	9.73	75.3	12.1	75.2
	5	12.2	78.2	14.9	78.2	9.62	75.2	10.9	75.2
	10	11.9	78.1			9.36	75.1		

provements we come up against an interesting situation in which, at the moment, a choice must be made concerning which physical characteristics are to be included in the theory. The principal deficiency of the present approach is that the ground-state charge density is taken to be constant at the bulk value right to the surface. In the real world, there will be a region over which the ground-state charge density goes from its bulk value to zero, perhaps including Friedel-like oscillations, and this structure in the charge density will affect the longitudinal field and, thus, the surface photoeffect. The importance of such effects in using the electron gas to stimulate the surface photoeffect for real systems is simply not known. Feibelman<sup>30</sup> has recently developed a self-consistent, surface photoeffect theory, including nonlocality, for the electron gas without damping. His procedure entails the assumption of a form for the surface potential, the calculation of wave functions consistent with this potential, the use of these wave functions in obtaining the nonlocal vector potential, and finally the calculation of surface-effect matrix elements using the interaction (5.2). In this way the effects associated with the charge rearrangement near the surface are included.

While Feibelman can treat rather well the undamped electron gas, the theory is of limited usefulness because damping effects will in general be of considerable importance for real systems. Writing, as we have, the theory in terms of the nonlocal dielectric functions means that damping effects can be incorporated with ease and various dielectric functions representing a variety of real physical effects (e.g., band structure) can be utilized.

For reasonably high energies,  $\omega$  of the order of 2 or 3 times the plasma frequency, both approaches suffer from a deficiency which may be serious. The vector potential for such frequencies varies considerably over several angstroms. In such cir-

cumstances, it is quite likely that the retention only of terms which are roughly macroscopic in character (corresponding to the diagonal elements of a dielectric tensor) is insufficient; local-field effects should be included. Neither the theory presented here nor the theory of Feibelman includes such effects.

An additional advantage of the approach presented here is the fact that the physics is rather more transparent, involving, as it does, familiar concepts such as the energy-loss function and the associated bulk excitations. This will be even more apparent when the energy- and angle-resolved photoyields are presented from the point of view presented here.<sup>51</sup> Furthermore, the present procedure can be used to discuss the surface photoeffect when the surface scattering of the internal electrons is other than specular. What is needed is a theory which includes the surface potential in a reasonable way (like that of Feibelman) but which also includes the flexibility of the present approach.

Finally, we would like to make several remarks about nondirect electronic transitions, the kind of transitions involved in the surface photoeffect. Although nondirect transitions occur, all nondirect transitions are not equally probable. The transition probabilities are weighted by the factor  $q^{-2}$ , where  $q$  is the magnitude of the momentum transfer. This means that small- $q$  transitions are very significantly favored over large- $q$  transitions. In addition, the relevant joint density of states cannot be obtained simply from energy considerations but requires a complicated analysis involving both energy and momentum.

#### ACKNOWLEDGMENT

I would like to thank Dr. E. Arakawa for providing me with the data used in the discussion of Sec. IV.

\*Prepared for the U. S. Energy Research and Development Administration under Contract No. W-7405-eng-82.

<sup>1</sup>G. Wentzel, Sommerfelds Festschrift, p. 79 (1928).

<sup>2</sup>I. Tamm and S. Shubin, Z. Phys. 68, 97 (1931).

<sup>3</sup>H. Fröhlich, Z. Phys. 75, 539 (1932).

<sup>4</sup>K. Mitchell, Proc. R. Soc. Lond. A 146, 442 (1934).

<sup>5</sup>K. Mitchell, Proc. R. Soc. Lond. A 153, 513 (1936).

<sup>6</sup>R. E. B. Makinson, Proc. R. Soc. Lond. A 162, 367 (1937).

<sup>7</sup>R. E. B. Makinson, Phys. Rev. 75, 1908 (1949).

<sup>8</sup>I. Adawi, Phys. Rev. 134, A788 (1964).

<sup>9</sup>G. D. Mahan, Phys. Rev. B 2, 4334 (1970).

<sup>10</sup>W. L. Schaich and N. W. Ashcroft, Phys. Rev. B 3,

2452 (1971).

<sup>11</sup>There is now an extensive literature concerning the bulk effect. Since the emphasis here is on the surface effect, no effort will be made to provide a complete list of references. A variety of theoretical perspectives is provided in the papers of Mahan (Ref. 9); Schaich and Ashcroft (Ref. 10); Gobel, Allen, and Kane (Ref. 12); Berglund and Spicer (Refs. 13 and 14); Puff (Ref. 15); Sass (Ref. 16); Caroli, Lederer-Rozenblatt, Roulet, and Saint-James (Ref. 17); and Feibelman and Eastman (Ref. 18a). Reference 18(b) includes a number of papers concerning various aspects of photoemission.

<sup>12</sup>G. W. Gobel, F. G. Allen, and E. O. Kane, Phys. Rev. Lett. 12, 94 (1964).

- <sup>13</sup>C. N. Berglund and W. E. Spicer, Phys. Rev. **136**, A1030 (1964).
- <sup>14</sup>C. N. Berglund and W. E. Spicer, Phys. Rev. **136**, A1044 (1964).
- <sup>15</sup>H. Puff, Phys. Status Solidi **1**, 636 (1961); **1**, 704 (1961).
- <sup>16</sup>J.-K. Sass, Surf. Sci. (to be published).
- <sup>17</sup>C. Caroli, D. Lederer-Rozenblatt, B. Roulet, and D. Saint-James, Phys. Rev. B **8**, 4552 (1973).
- <sup>18</sup>(a) P. Feibelman and D. Eastman, Phys. Rev. B **10**, 4932 (1974). (b) in *Vacuum Ultraviolet Radiation Physics*, edited by E.-E. Koch, R. Haensel, and C. Kunz (Vieweg, Braunschweig, 1974).
- <sup>19</sup>V. P. Silin and E. P. Fetisov, Zh. Eksp. Teor. Fiz. **41**, 159 (1961) [Sov. Phys.-JETP **14**, 115 (1962)].
- <sup>20</sup>A. M. Fedorchenko, Zh. Tekh. Fiz. **32**, 589 (1962) [Sov. Phys.-Tech. Phys. **7**, 428 (1962)].
- <sup>21</sup>A. M. Fedorchenko, Zh. Tekh. Fiz. **36**, 1327 (1966) [Sov. Phys.-Tech. Phys. **11**, 992 (1967)].
- <sup>22</sup>F. Sauter, Z. Phys. **203**, 488 (1967).
- <sup>23</sup>F. Forstmann, Z. Phys. **203**, 495 (1967).
- <sup>24</sup>K. L. Kliewer and R. Fuchs, Phys. Rev. **172**, 607 (1968).
- <sup>25</sup>R. Fuchs and K. L. Kliewer, Phys. Rev. **185**, 905 (1969).
- <sup>26</sup>V. P. Silin and E. P. Fetisov, Phys. Status Solidi **39**, 49 (1970).
- <sup>27</sup>A. R. Melnyk and M. J. Harrison, Phys. Rev. B **2**, 835 (1970).
- <sup>28</sup>A. R. Melnyk and M. J. Harrison, Phys. Rev. B **2**, 851 (1970).
- <sup>29</sup>K. L. Kliewer, Phys. Rev. Lett. **33**, 900 (1974).
- <sup>30</sup>P. Feibelman, Phys. Rev. Lett. **34**, 1092 (1975).
- <sup>31</sup>J. G. Endriz, Phys. Rev. B **7**, 3464 (1973).
- <sup>32</sup>Little physical significance can be attributed to the isotropic volume effect model unless the energy is high,  $\hbar\omega \gg E_F$ , where  $E_F$  is the Fermi energy. However, this model affords a particularly convenient and effective comparison with the nonlocal theory to be described below.
- <sup>33</sup>S. V. Pepper, J. Opt. Soc. Am. **60**, 805 (1970).
- <sup>34</sup>J. G. Endriz and W. E. Spicer, Phys. Rev. B **4**, 4159 (1971).
- <sup>35</sup>P. Vernier, J. P. Goudonnet, G. Chabrier, and J. Cornaz, J. Opt. Soc. Am. **61**, 1065 (1971).
- <sup>36</sup>Essentially all of the results in Refs. 19–28 involve, explicitly or implicitly, the assumption of specular scattering.
- <sup>37</sup>N. D. Mermin, Phys. Rev. B **1**, 2362 (1970).
- <sup>38</sup>This is true only for specular scattering.
- <sup>39</sup>K. L. Kliewer and R. Fuchs, Phys. Rev. **181**, 552 (1969).
- <sup>40</sup>(a) An example is silver. See P. Zacharias and K. L. Kliewer, Solid State Commun. **18**, 23 (1976). (b) Note that this result is in no way dependent upon the re-

placement of the transverse dielectric function by its local value. The general expression for  $E_z(z)/H_y(0)$  is Eq. (2.17b) plus  $F(z)$ ,

$$F(z) = \frac{2\omega^2\epsilon_0^{1/2}\sin\theta}{\pi c^2} \int_0^\infty \frac{dq_z q_z \sin(q_z z)}{q^2} \times \left[ \frac{1}{(\omega^2/c^2)\epsilon_{t,T} - q^2} - \frac{1}{(\omega^2/c^2)\epsilon_T - q^2} \right],$$

where  $\epsilon_{t,T}$  is the general,  $q$ -dependent transverse dielectric function which includes the local contribution  $\epsilon_{ex}(\omega)$ . In the limit  $z \rightarrow 0$ ,  $F(z) \rightarrow 0$ .

<sup>41</sup>We are interested here only in  $\omega \geq 0$  and  $q \geq 0$ .

<sup>42</sup>K. L. Kliewer and H. Raether, J. Phys. C **7**, 689 (1974).

<sup>43</sup>Keep in mind that the contribution to  $dA/dz$  from the  $z$  components is zero at the surface since  $J_z(0) = 0$  for the electron gas in the nonlocal description.

<sup>44</sup>At  $z = 0$ , the field ratio is given rigorously by Eq. (2.18), a result  $\sim 1$ . Both terms in Eq. (3.6) are  $\sim 1/\epsilon$ . Since we are here in the region where  $\epsilon \sim 0$ , the discrepancy between (3.5) and (2.18) is not of serious consequence. Clearly, the present argument is only valid for  $\omega$  close to  $\omega_p$  where  $\epsilon \approx 0$ .

<sup>45</sup>Endriz (Ref. 31) noted the reduction of the photoyield associated with the reactive longitudinal effects but ignored the more important resistive effects.

<sup>46</sup>The restriction to negative  $\epsilon$  is important. For  $\omega < \omega_p$ ,  $q_R$  is essentially imaginary and describes the suppression of the total field. For  $\omega > \omega_p$ ,  $q_R$  is essentially real and describes the propagating plasmon. The role of the plasmon in photoemission is discussed below.

<sup>47</sup>J. M. Keller, R. Fuchs, and K. L. Kliewer, Phys. Rev. B **12**, 2012 (1975).

<sup>48</sup>E. T. Arakawa, R. N. Hamm, and M. W. Williams, J. Opt. Soc. Am. **63**, 1131 (1973).

<sup>49</sup>K. L. Kliewer, Ref. 18b, p. 575.

<sup>50</sup>These curves involve the same parameters for which curves of  $dA/dz$  were given in Ref. 29.

<sup>51</sup>K. L. Kliewer (unpublished).

<sup>52</sup>J. P. Goudonnet, G. Chabrier, and P. J. Vernier, Ref. 18b, p. 577.

<sup>53</sup>E. T. Arakawa, M. W. Williams, R. N. Hamm, R. D. Birkhoff, and A. J. Braundmeier, Ref. 18b, p. 580.

<sup>54</sup>E. T. Arakawa (private communication).

<sup>55</sup>C. R. Brundle, J. Vac. Sci. Technol. **11**, 212 (1974).

<sup>56</sup>C. J. Powell, Surf. Sci. **44**, 29 (1974).

<sup>57</sup>H. Becker, E. Dietz, U. Gerhardt, and H. Angermüller, Phys. Rev. B (to be published).

<sup>58</sup>J.-K. Sass (private communication).